Determination of the α, β, and γ Crystalline Phases of Poly(vinylidene fluoride) Films Prepared at Different Conditions

Rinaldo Gregorio, Jr.

Department of Materials Engineering, Universidade Federal de São Carlos, CP 676, CEP 13.565–905, São Carlos, São Paulo, Brazil

Received 7 June 2005; accepted 1 September 2005
DOI 10.1002/app.23137
Published online in Wiley InterScience (www.interscience.wiley.com).

ABSTRACT: Samples containing the three crystalline phases of poly(vinylidene fluoride), α, β, and γ, have been obtained under distinct crystallization conditions. Samples containing exclusively unoriented β phase have been obtained by crystallization from dimethylformamide (DMF) solution at 60°C. Oriented β phase has been obtained by uniaxial drawing, at 80°C, of an originally α phase sample. Samples containing exclusively α phase have been obtained by melting and posterior cooling at room temperature. Samples containing both α and γ phases have been obtained by melt crystallization at 164 °C for 16 and 36 h. Presence of the crystalline phases in each sample were confirmed by Fourier transform infrared spectroscopy (FTIR), differential scanning calorimetry (DSC), wide-angle X-ray scattering (WAXD), polarized light optical microscopy (PLOM), and scanning electron microscopy (SEM). Infrared absorption bands identifying unequivocally the presence of β and γ phases in a sample are presented. It is shown that solution crystallization at $T < 70$°C always results in the β phase, regardless of the solvent used. Melt temperatures of the respective phases have also been determined. © 2006 Wiley Periodicals, Inc. J Appl Polym Sci 100: 3272–3279, 2006

Key words: PVDF; crystalline phase; crystallization; spherulites; FTIR

INTRODUCTION

Poly(vinylidene fluoride) PVDF, has been extensively investigated during the last three decades mainly because of its unequaled properties. PVDF can be easily processed, and has excellent mechanical properties, high chemical resistance, good thermal stability as well as high pyro and piezoelectric coefficients. These properties provide a wide range of scientific as well as technological applications,[1–3] from simple protective coatings for pipes and buildings to transducer devices, detectors, ferroelectric memories, etc. Recently, PVDF has also found several applications in biomedicine. However, technological improvement of these devices depends on film processing techniques of which the properties are well known, optimized, and reproducible. This requires a better understanding of the effect of processing on the type of crystalline phase obtained, as this determines the material properties. As an example, we may cite the pyro and piezoelectric applications of PVDF, which are believed to be intimately related to the polar crystalline phase, known as β (or I). In addition to this phase, PVDF can also crystallize into at least two other phases: a nonpolar one, known as α (or II) and another polar one, known as γ (or III). Conformation and structure of these three phases, as well as, their characteristic infrared absorption bands and the associated vibration modes are extensively documented in the literature.[4–10]

As to the obtainment of each phase, the α phase is more easily obtained, always resulting from melt crystallization at any temperature. For films cast from an appropriate solution, this phase predominates if evaporation occurs at temperatures above 110°C[8] Temperatures between 70 and 110°C result in a mixture of α and β and temperatures below 70°C result exclusively in the β phase. Oriented β phase can be obtained by mechanical drawing, either uniaxial or biaxial, of films originally in the α phase at temperatures between 70 and 90°C. Drawing at temperatures above 120°C result in the oriented α phase.[9] The γ phase may be obtained (either from the melt or solution casting) by crystallizing at temperatures near the melt temperature (T_m) of the α phase.[8,10–12] Annealing at temperatures close to T_m also result in the γ phase, because of $\alpha \rightarrow \gamma$ solid state phase transformation.[10,12–14] A great number of works have been published on the obtainment and characterization of the different PVDF phases, showing many conflicting results. Recent works[15–19] have shown that low-temperature solution

Correspondence to: R. Gregorio, Jr. (gregorio@power.ufscar.br).
Contract grant sponsors: CNPq, PADCT III/Milênio, and PRONEX.

crystallization ($T < 70$°C) results in α or γ phase or even a mixture of these, depending on the type of solvent used, contradicting results obtained by other authors who state that under these conditions the β phase should predominate.[8,9] These divergent results occur largely because the main characterization technique employed is FTIR and some characteristic absorption bands of the β and γ phases either coincide or are so close to each other that they can not be distinguished. In addition, some authors still confuse the melt temperature corresponding to each phase.[16,20,21]

The aim of this study was to show in an unequivocal way which infrared absorption bands are characteristic of each phase, and how each processing technique may lead to a single phase or a mixture of phases. To this end PVDF films at the different phases were obtained through distinct processing techniques and characterized by FTIR spectrometry, differential scanning calorimetry (DSC), Wide-angle X-ray diffraction (WAXD), and optical and electronic microscopy. Melt temperatures of the three crystalline phases were also determined.

EXPERIMENTAL

Materials and sample preparation

The following processing techniques have been used:

i. Films of 3 and 15 μm thickness were obtained by solution casting. A PVDF (FORAFLON F4000-Atochem)/dimethylformamide (Merk, 99.5%) solution was spread on a clean glass substrate by means of a metallic blade. Initial solution concentration was 20 wt % PVDF. Solvent evaporation was carried out at 60°C on a temperature-controlled hot plate inside a fume hood. After complete evaporation of the solvent, within 60 min, the system was immersed in distilled water at room temperature (25°C) allowing facile removal from the substrate. This sample was denominated as sample A.
ii. Sample A was melted at 220°C for 10 min on the glass substrate and left to cool at room temperature, resulting in sample B.
iii. Sample B was uniaxially drawn at 80°C at draw ratios (relation between initial and final sample length) of 3 and 4. The draw velocity used was 3 mm/min.
iv. Sample B was melted at 220°C for 10 min, subsequently quenched (20°C/min) at 166°C, and left to crystallize isothermally for 16 and 36 h. After this period the sample was quenched in an ice-distilled water bath.

Characterization techniques

FTIR spectra were obtained in a Perkin–Elmer Spectrum 1000 spectrometer with resolution of 2 cm^{-1}. Spectra were taken under scanning with a diaphragm of 2 mm diameter. Calorimetric measurements (DSC) were carried out in a TA Instruments Q100 equipment, at a heating rate of 10°C/min. Wide-angle X-ray diffraction (WAXD) was done in a Rigaku Rotaflex RU-200B diffractometer. Optical microscopy images were obtained in a Leica DMRXP optical microscope with polarized light and in a Philips XL30-FEG scanning electronic microscope.

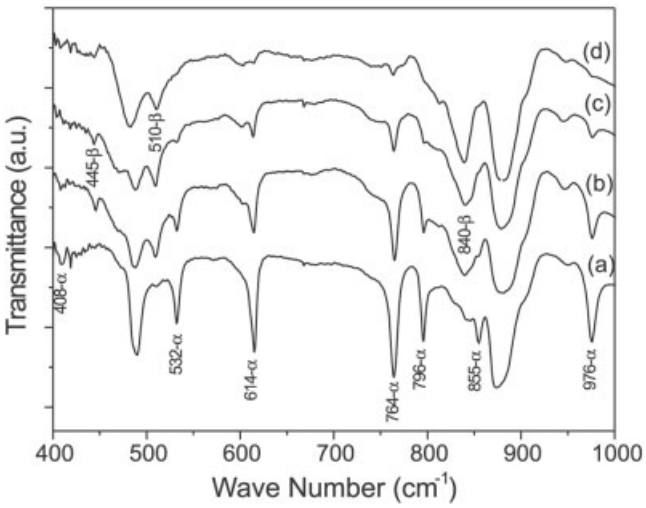

Figure 1 FTIR transmission spectra of sample B (a), of sample B drawn at 80°C with ratio of 3 (b) and 4× (c) and of sample A (d).

RESULTS

IR spectroscopy

FTIR spectra of sample B undrawn, and at a draw ratio of 3 and 4 are shown in Figure 1(a–c). Sample B, melted and subsequently cooled to room temperature, shows the characteristic spectrum of the α phase, with well-defined absorption bands at 408, 532, 614, 764, 796, 855, and 976 cm^{-1}. As draw ratio increases the intensity of the characteristic α phase bands decreases and that of the bands at 445, 510, and 840 cm^{-1}, characteristic of the β phase, increases. This was as expected; several investigation have reported that drawing of α phase samples at 80°C causes $\alpha \rightarrow \beta$ transformation.[9,22] Even at a draw ratio of 4, the 532, 614, 764, and 976cm^{-1} bands can still be seen, indicating that the α phase continues to be present in the sample. The same figure also shows the spectrum of sample A [Fig. 1(d)]. The 510 and 840 cm^{-1} bands, characteristic of the β phase, can be clearly seen, however virtually no considerable band corresponding to the α phase. Hence, it seems evident that the solution crystallized sample at 60°C presents almost exclusively the β phase. This result corroborates those ob-

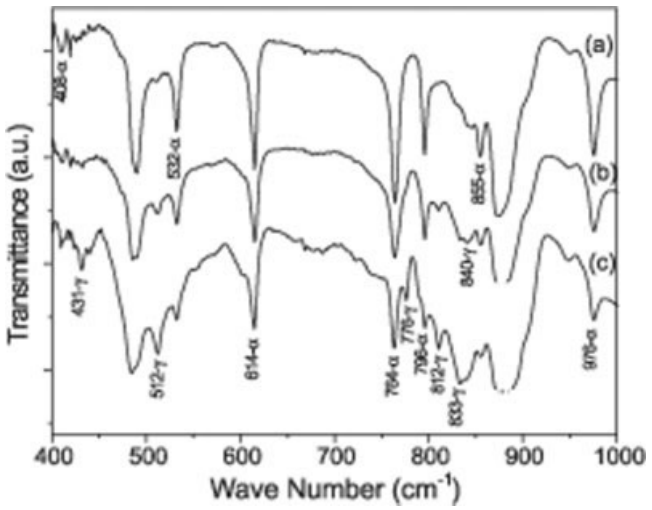

Figure 2 FTIR transmission spectra of sample B (a) and of sample B after melting and crystallization at 166°C for 16 h (b) and 36 h (c).

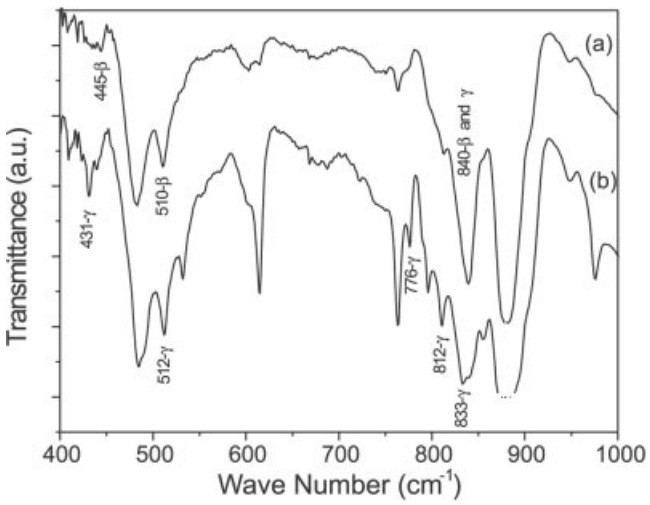

Figure 3 FTIR transmission spectra of sample A (a) and of sample B after melting and crystallization at 166°C for 36 h (b).

tained in previous works[8,9,23] and will be confirmed by X-ray diffraction and DSC.

Figure 2(a–c) shows IR spectra of sample B, before and after melting and subsequent isothermal crystallization at 166°C for 16 and 36 h. It can be seen that increase in crystallization time results in a decrease in intensity of the characteristic α phase bands (408, 532, 614, 764, 796, 855, and 976 cm^{-1}) and an increase in those characteristic of the γ phase (431, 512, 776, 812, 833, and 840 cm^{-1}). This result was also as expected from results in the literature, which shows that crystallization of PVDF for long periods and at temperature close to T_m of the α phase results in the γ phase.[8,10–13] This phase may either crystallize directly from the melt or be formed from $\alpha \rightarrow \gamma$ solid phase transformation. However, it is of importance that the γ phase presents some characteristic bands very distinct from those presented by the β phase. The 840 cm^{-1} band is common to both phases, and the 512 band is very close to the 510 cm^{-1} band of the β phase. However, the 431, 776, 812, and 833 cm^{-1} bands are exclusively of the γ phase, and the 445 cm^{-1} band is exclusively of the β phase. Figure 3(a,b) shows the spectra of sample A and sample B after crystallization at 166°C for 36 h. Despite containing a mixture of the α and γ phases, and therefore still presenting several characteristic α phase bands, the sample crystallized at 166°C evidences the clear difference between the characteristic β and γ phase bands. It is also evident that the 840 cm^{-1} band is common to the two phases (in the case of the γ phase it can be seen as a shoulder of the 833 cm^{-1} band) and can be well distinguished from the 833 cm^{-1} band, exclusively of the γ phase, in a spectrophotometer with 2 cm^{-1} resolution. Therefore, to distinguish unequivocally between β and γ phase in a sample, one should look for the existence or not of the 431, 776, 812, and 833 cm^{-1} bands, exclusively of the γ phase. Figure 4 presents the same spectra shown in Figure 3, however, for very thin samples (~3 μm). The 1234 cm^{-1} band, which can be seen only in very thin samples due to the intense absorption in the 1150–1250 cm^{-1} region, which some authors attribute to the γ phase exclusively as γ,[16,17,19] is common to the β and γ phase, and therefore should not be considered for distinguishing these phases. In this figure another band at 1117 cm^{-1} can be seen as well, which also seems to be characteristic of the γ phase. In addition to these differences between the absorption bands of β and γ phases, the following should be considered. The β phase is formed from solution crystallization at low temperature ($T \leq 90$°C),

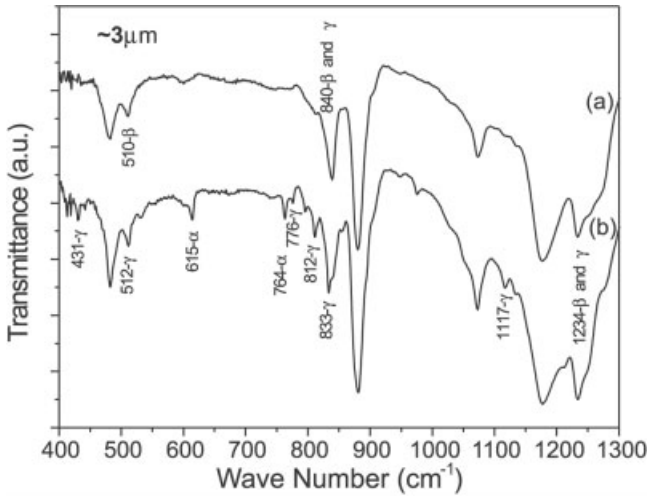

Figure 4 FTIR transmission spectra of sample A (a) and of sample B after melting and crystallization at 166°C for 36 h (b) for thin films (~3 μm).

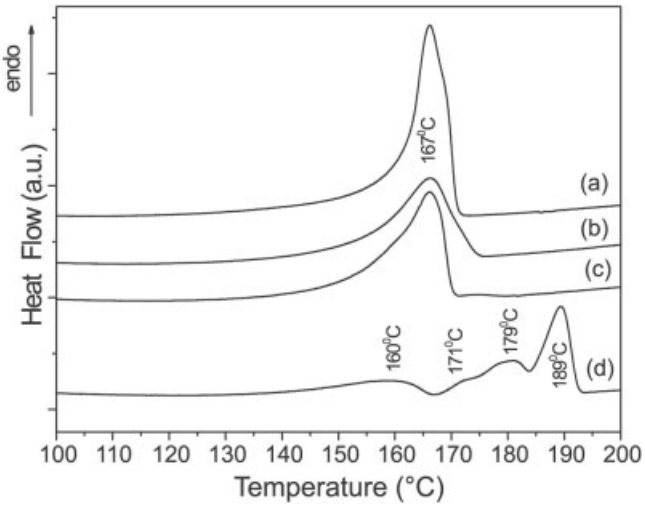

Figure 5 DSC curves of sample B (a), sample B after drawing at 80°C at a draw ratio of 4 (b), sample A (c) and sample B after melting and crystallization at 166°C for 36 h (d).

predominating at $T < 70$°C. It can be obtained by drawing originally α phase samples at temperatures below 90°C or still by ultra quenching from the melt, only possible for very thin films.[24] The γ phase, on the other hand, is only formed by crystallization or annealing at high temperatures, close to T_m of the α phase. Therefore, it is not possible to form these two phases simultaneously from crystallization, neither from the melt nor from solution.

Thermal analyses

Figure 5 shows DSC curves of samples A (c), B (a), B after drawing at 80°C with a draw ratio of 4 (b) and B after isothermal crystallization at 166°C for 36 h (d). The melt temperatures (represented by the endothermal peak) of the phases α (a) and β (b e c) are seen to coincide at 167°C, as already reported in a previous investigation.[8] The similarity of the thermograms of sample A (c) and of sample B after drawing (b) should also be noted, demonstrating again that the phase obtained from solution crystallization at 60°C is indeed the β phase. The thermogram of sample B crystallized for 36 h at 166°C (d) shows 3 endotherms, in addition to a shoulder at 171°C. The peak at 160°C corresponds to fusion of the α phase consisting of very small spherulites (~8 μm), crystallized from quenching the sample after isothermal crystallization at 166°C. The endotherm with a peak at 179°C corresponds to the fusion of the γ phase crystals formed from the melt at 166°C, which predominates in the nonringed spherulites and which will be dealt in the following section. The endotherm at 189°C corresponds to the fusion of the γ phase crystals formed from the $\alpha \rightarrow \gamma$ solid state phase transformation, which occurs in the ringed spherulites, originally formed by the α phase, and which will also be dealt in the following section. The small shoulder at the onset of the endotherm at 179°C, with the peak at about 171°C, likely corresponds to the fusion of the α phase crystallized at 166°C for 36 h, forming the ringed spherulites that did not undergo the $\alpha \rightarrow \gamma$ transformation. These results agree with those obtained in previous work[10] and confirm that the sample crystallized from solution at 60°C consists predominantly of the β phase. The melt temperatures of the β and γ phases, sometimes confused by a few investigators,[16,20,21,25] are also confirmed. Obviously, the melt temperatures corresponding to the several PVDF phases are of the F4000 of Atochem resin. T_m of each phase depends on the polymerization conditions and, therefore, on the resin used. However, in any way, the melt temperatures of α and β phases virtually coincide, for α crystallized from the melt at $T < 140$°C (T_m of the α phase increases with increasing crystallization temperature). In the same sample, T_m of the γ phase crystallized from the melt is about 8°C higher than that of the α phase, and T_m of the γ phase formed by the $\alpha \rightarrow \gamma$ transformation is about 18°C higher than that of the α phase.

Microscopy

Solution crystallized sample at 60°C presented a porous structure formed by spherulites with a diameter between 3 and 6 μm, as shown by the SEM micrograph in Figure 6. This structure renders whitish translucent films becoming milky opaque when thicker. This occurs because the cavities between the solid/air interface reflect and refract the visible radiation and even infrared in the range of 2000–4000 cm^{-1} range, causing a slope in the spectrum base line, as shown by Benz and coworkers.[26] This porosity may be useful in PVDF membrane applications, however, it

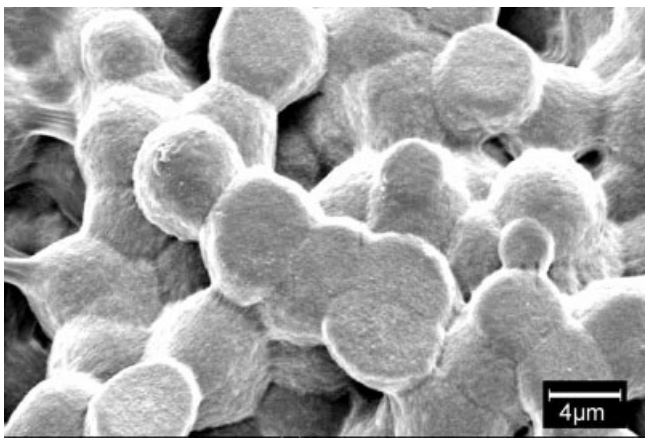

Figure 6 SEM micrograph of sample A.

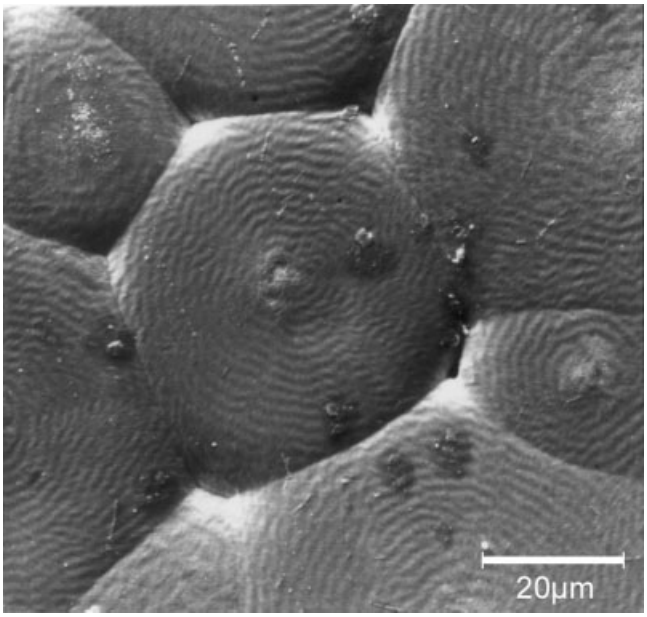

Figure 7 SEM micrograph of sample B.

reduces mechanical strength of these films rendering them little ductile. For this reason, sample A was melted and cooled before drawing to avoid tearing during the process. Another problem caused by the high porosity of these films occurs during polarization: they break at relatively low electric fields, encumbering the polarization process. At present our research group is making efforts to obtain porosity-free unoriented β phase films. The size of solution crystallized spherulites depends on temperature, and for thin films may also depend on the substrate used. With increasing temperature spherulite diameter increases[8,9] and the sample becomes less porous, however, α phase formation increases. Samples crystallized at 140°C are transparent; however, they consist predominantly of the α phase. Figure 7 shows a SEM micrograph of sample B, melted and cooled to room temperature. Under these conditions crystallization likely occurred between 130 and 140°C[8] forming ringed spherulites with diameter between 20 and 40 μm and containing predominantly the α phase. This sample showed to be very transparent, flexible and of excellent mechanical strength, which facilitated drawing. Figure 8 depicts a micrograph of sample B after drawing at 80°C at a ratio of 4, showing the oriented fibril structure of this sample. The β phase may thus either present spherulites, when obtained from solution, or oriented fibrils.

Figure 9 depicts a polarized light optical micrograph of sample B after fusion and crystallization for 36 h at 166°C, showing ringed and nonringed spherulites as already described in previous works.[8,10,12,27] The ringed spherulites are formed by melt crystallization and contain predominantly the α phase. The non-

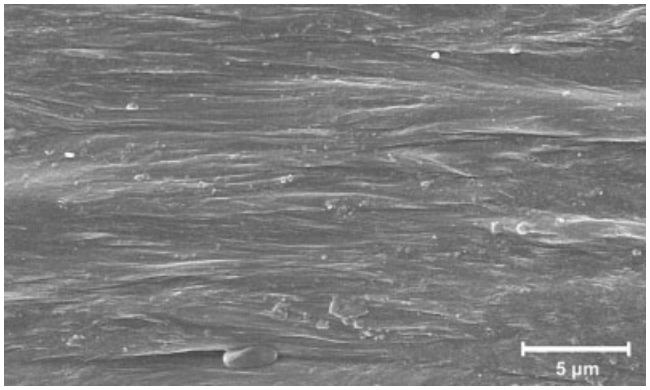

Figure 8 SEM micrograph of sample B after drawing at 80°C with draw ratio of 4.

ringed spherulites, containing the γ phase with small α phase inclusions, are also formed from melt crystallization, however only when this occurs at temperature close to T_m of the α phase (in the case of Atochem F4000 resin, at $T > 155$°C). These spherulites lose birefringence between 178 and 184°C, confirming that this is the melt temperature range of the γ phase crystallized directly from the melt. When the sample remains at temperature close to α phase T_m a solid state $\alpha \rightarrow \gamma$ phase transformation takes place in the ringed spherulites. Part of the spherulites that experienced this transformation lost birefringence only between 188 and 193°C, confirming that this is the melt of the γ phase formed from α phase transformation. A detailed investigation on solid state $\alpha \rightarrow \gamma$ phase transformation has been published in previous work.[10]

X-ray diffraction

Figure 10 shows diffractograms of samples A (c), B (a), B drawn at 80°C at a draw ratio of 4 (d) and B after

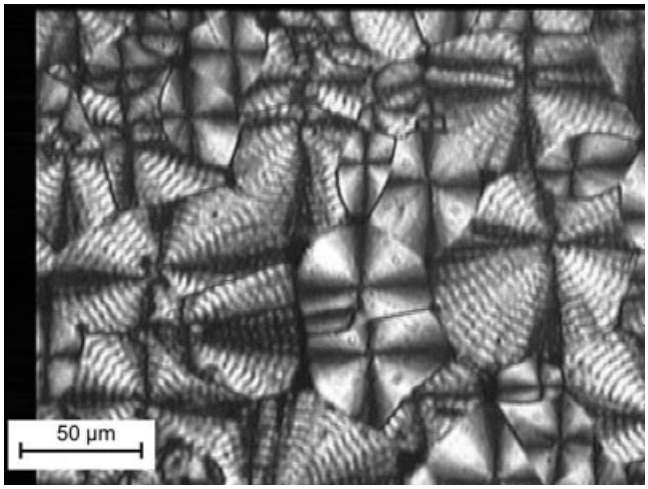

Figure 9 Polarized light optical micrograph of sample B after melting and crystallization at 166°C for 36 h.

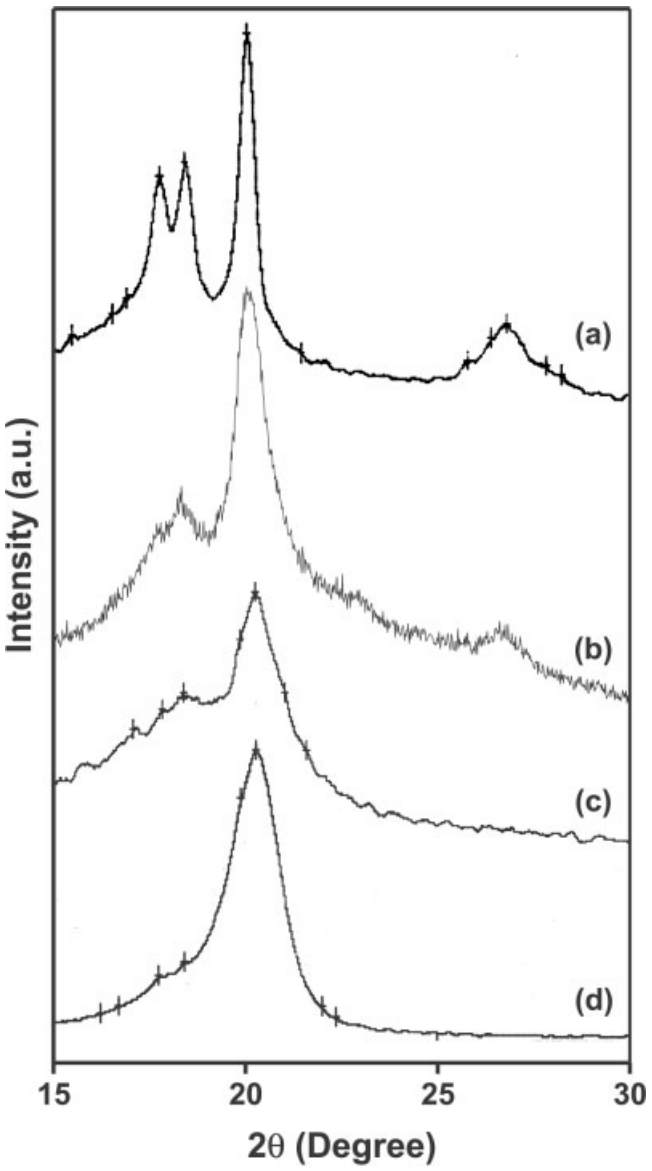

Figure 10 X-ray diffractograms of sample B (a), sample B after melting and crystallization at 166°C for 36 h (b), sample A (c) and sample B drawing at 80°C at draw ratio of 4 (d).

crystallizing for 36 h at 166°C (b). Table I lists values of 2θ and of interplanar spacing d corresponding to the peaks observed in the diffractograms of Figure 10. The spectra of sample A (c) and sample B after drawing (d) are seen to have a well defined peak at $2\theta = 20.26°$, referent to the sum of the diffractions in plane (110) and, (200) characteristic of the β phase,[9,28] confirming again the obtainment of this phase during solution crystallization at 60°C. The diffractogram of sample B (a) presents peaks at $2\theta = 17.66$, 18.30, 19.90, and 26.56°, referent to the diffractions in planes,(100), (020), (110), and (021) respectively, all characteristic of the α phase,[9,28] confirming observations by FTIR. The diffractogram of sample B crystallized for 36 h at 164°C (b) is expected to present peaks characteristic of α and γ phases, since observations by FTIR and DSC of this sample indicated a mixture of these phases. Unfortunately, as far as we know, until now no characteristic diffractogram of a sample containing exclusively the γ phase has been obtained yet and, therefore, the characteristic peaks of this phase are unknown. This is due to samples containing the γ phase that always contain a large amount of the α phase. Even samples remaining at 130 h at 166°C still presented FTIR absorption bands characteristic of both phases. This occurs because the nonringed spherulites, crystallized at elevated temperatures and containing predominantly the γ phase, always present α phase inclusions.[10,12] The $\alpha \rightarrow \gamma$ transformation occurring in the ringed spherulites at high temperature seems to be never complete. A portion of the α phase always remains in these spherulites.[10] This way, the diffractogram presented in Figure 10(b) is expected to contain peaks corresponding to both α and γ phases. Indeed, peaks are seen at $2\theta = 17.66$, 18.3, and 26.56°, all characteristic of the α phase. A somewhat more intense peak can also be seen at $2\theta = 20.04°$, resulting likely in the superposition of the α phase peak at 19.90° and the peak characteristic of the γ phase, of which the 2θ value is unknown. At present, our group is attempting to obtain films with as much γ phase as possible to be able to obtain a diffractogram of this phase.

DISCUSSION

This investigation confirms that crystallization from DMF solution at $T < 70$°C results predominantly in formation of the β phase, results that are already obtained in previous works.[8,9,23,29,30] Films crystallized from DMA solution also presented the same results.[8] Few authors reported obtainment of α or γ phase during solution crystallization at $T < 80$°C, depending on the solvent or substrate used[4,14–19,21] Very polar liquids such as dimethylsulfoxide (DMSO),

TABLE I
Values of 2θ and Respective d Spacing Observed in the Diffractograms of Figure 10

	2θ	d (Å)
Phase α (Fig. 10a)	17.66	5.018
	18.30	4.844
	19.90	4.458
	26.56	3.353
Phase β (Figs. 10c, 10e, and 10d)	—	—
	—	—
	20.26	4.38
	—	—
Phases $\alpha + \gamma$ (Fig. 10b)	17.66	5.018
	18.30	4.844
	20.04	4.427
	26.56	3.35

N,*N*-dimethylformamide (DMF), *N*-methyl-2-pyrrolidone (NMP), hexamethylphosphoramide (HMPA) and *N*,*N*-dimethylacetamide (DMA), would result in the γ phase, whereas liquids like ethanol, cyclohexanone, and toluene would result in the α phase. Other solvents like tetrahydrofuran (THF), methyl ethyl ketone (MEK), and acetone would yield either γ phase or a mixture of α and γ phases. However, infrared analysis by these authors did not show the absorption bands at 431, 776, 812, and 833 cm^{-1}, which unequivocally characterize the γ phase. To characterize this phase they used the 840 and 1234 cm^{-1} bands, which as we have seen are common to both phases. Therefore, likely on using strongly polar solvents, on dissolving the crystalline phase the phase obtained by these authors was the β and not the γ phase. When other less polar solvents were used, dissolution of the crystalline phase might not have occurred or dissolution might have been incomplete. Dissolution of the PVDF crystalline regions requires polymer–solvent interaction energy exceed that between the polymer chains. When this does not occur the crystalline region remains practically unaltered and the polymer will swell, because of solvent penetration into the amorphous phase. Temperature increase may reduce chain interaction, allowing solvent penetration into the crystalline region. Bottino and coworkers[31] investigated PVDF solubility in several liquids. They observed that liquids like DMA, DMF, DMSO, HMPA, NMP, tetramethylurea (TMU), triethylphosphate (TEP), and trimethylphosphate (TMP) manage to penetrate and dissolve the crystalline region of PVDF at 60°C. These solvents were considered good solvents of this polymer. Other liquids like THF, MEK, cyclohexanone, and acetone were considered good swelling agents, that is, at 60°C they manage to penetrate the amorphous phase, strongly swell the polymer and may partially dissolve the crystalline phase. Others like ethanol were considered poor swelling agents or nonsolvents. In this case, the liquids promote only slight swelling of the polymer without practically affecting the crystalline phase. If we look at the solvents used by the authors in the aforementioned works[4,14–19,21] it can be seen that when good solvents were used, they stated that PVDF crystallization at 60°C resulted in the γ phase. The crystalline part of the polymer dissolved and crystallized during solvent evaporation at 60°C. However, we believe that the phase formed in this case was the β phase and not the γ phase. When good swelling agents were used, they stated that an α phase resulted, or still a mixture of α and γ, which we believe have been α and β. In this case the liquid dissolved only part of the original α phase of the sample that, during evaporation at 60°C, crystallized into the β phase. The result was a mixture of the α phase, which did not undergo dissolution, and the β phase. When the liquid used was a poor swelling agent or nonsolvent, the crystalline part originally in the α phase remained practically intact, resulting in this same phase.

We are convinced that solution crystallization at $T < 70$°C will always result predominantly in formation of the β phase, regardless of the solvent used, provided it is a good solvent for PVDF. As temperature increases α phase formation increases, becoming predominant at $T > 110$°C. The γ phase can only be obtained (either from the melt or from solution with a good solvent), when crystallization occurs at temperatures near T_m of the α phase, or on annealing, also at high temperature, of a sample originally in the α phase. In the former case, application of an electric field (~70 kV/cm) may favor formation of the γ phase.[32]

CONCLUSIONS

Crystallization of PVDF from solution at $T < 70$°C always results exclusively in β phase, regardless of the solvent used, as long as it is a good solvent for this polymer. Increase in temperature increases α phase formation, becoming predominant at $T > 110$°C. The γ phase is only obtained during crystallization either from the melt or from solution at temperatures close to T_m of the α phase, or by annealing an originally α phase sample at these temperatures. To unequivocally distinguish the β and γ phases in a sample employing FTIR, one should attend to the presence or not of the absorption bands at 431, 776, and 812 cm^{-1}, exclusively of the γ phase, and of the 445 cm^{-1} band, exclusively of the β phase. The 833 cm^{-1} band, although exclusively of the γ phase, may be confused with the 840 cm^{-1} band, which is common to both the phases. The 1234 cm^{-1} band is also common to both phases. The β phase melt temperature practically coincides with that of the α phase crystallized at $T < 140$°C. In a same sample melt temperature of the γ phase crystallized from the melt, forming nonringed spherulites, is about 8°C higher than the T_m of the α phase. Melt temperature of the γ phase formed from the $\alpha \rightarrow \gamma$ transformation, which occurs at high temperature in the ringed spherulites is about 18°C higher than the T_m of the α phase crystallized at this temperature.

References

1. Chen, Q. X.; Payne, P. A. Meas Sci Technol 1995, 6, 249.
2. Seiler, D. A. In: Modern Fluoropolymers, 2nd ed.; Scheirs, J., Ed.; Wiley: Chichester, 1998; p 487.
3. Reece, T. J.; Ducharme, S.; Sorokin, A. V.; Poulsen, M. Appl Phys Lett 2003, 82, 142.
4. Kobayashi, M.; Tashiro, K.; Tadokoro, H. Macromolecules 1975, 8, 158.
5. Broadhurst, M. G.; Davis, G. T.; McKinney, J. E.; Collins, R. E. J Appl Phys 1978, 49, 4992.

6. Davis, G. T. In The Applications of Ferroelectric Polymers; Wang, T. T.; Herbert, J. M.; Glass, A. M., Eds.; Blackie & Sons: London, 1988; p 37.
7. Lovinger, A. J. In: Developments in Crystalline Polymers; Basset, D. C., Ed.; Applied Science Publications: London, 1981; p 195.
8. Gregorio, R., Jr.; Cestari, M. J Polym Sci Part B: Polym Phys 1994, 32, 859.
9. Gregorio, R., Jr.; Ueno, E. M. J Mater Science 1999, 34, 4489.
10. Gregorio R., Jr.; Capitão, R. C. J Mater Sci 2000, 35, 299.
11. Osaki, S.; Ishida, Y. J Polym Sci Polym Phys Ed 1975, 13, 1071.
12. Lovinger, A. J. J Polym Sci Polym Phys Ed 1980, 18, 793.
13. Prest, W. M., Jr.; Luca, D. J. J Appl Phys 1978, 49, 5042.
14. Bachmann, M. A.; Gordon, W. L.; Koenig, J. L.; Lando, J. B. J Appl Phys 1979, 50, 6106.
15. Abbrent, S.; Plestil, J.; Hlavata, D.; Lindgren, J.; Tegenfeldt, J.; Wendsjö, A. Polymer 2001, 42, 1407.
16. Benz, M.; Euler, W. B. J Appl Polym Sci 2003, 89, 1093.
17. Boccaccio, T.; Bottino, A.; Capannelli, G.; Piaggio, P. J Membr Sci 2002, 210, 315.
18. Benz, M.; Euler, W. B.; Gregory, O. J. Macromolecules 2002, 35, 2682.
19. Park, Y. J.; Kang, Y. S.; Park, C. Eur Polym J 2005, 41, 1002.
20. El Mohajir, B.; Heymans, N. Polymer 2001, 42, 5661.
21. Lee, W. K.; Ha, C. S. Polymer 1998, 39, 7131.
22. Sajkiewicz, P.; Wasiak, A.; Goclowski, Z. Eur Polym J 1999, 35, 423.
23. Gregorio R., Jr.; Nocite, N. C. P. S. J Phys D: Appl Phys 1995, 28, 432.
24. Hsu, C. C.; Geil, P. H. J Appl Phys 1984, 56, 2404.
25. Scheinbeim, J.; Nakafuku, C.; Newman, B. A.; Pae, K. D. J Appl Phys 1979, 50, 4399.
26. Benz, M.; Euler, W. B.; Gregory, O. J Langmuir 2001, 17, 239.
27. Prest, W., Jr.; Luca, D. J. J Appl Phys 1975, 46, 4136.
28. Davis, G. T.; McKinney, J. E.; Broadhurst, M. G.; Roth, S. C. J Appl Phys 1978, 49, 4998.
29. Gregorio R., Jr.; Cestari, M.; Bernardino, F. E. J Mater Sci 1996, 31, 2925.
30. Rocha, I. S.; Mattoso, L. H. C.; Malmonge, L. F.; Gregorio R., Jr. J Polym Sci Part B: Polym Phys 1999, 37, 1219.
31. Bottino, A.; Capannelli, G.; Munari, S.; Turturro, A. J Polym Sci Part B: Polym Phys 1988, 26, 785.
32. Marand, H. L.; Stein, R. S.; Stack, G. M. J Polym Sci Part B: Polym Phys 1988, 26, 1361.